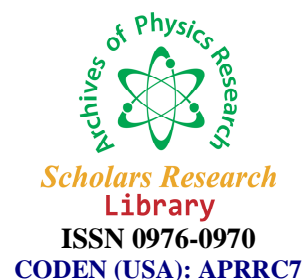




Scholars Research Library

Archives of Physics Research, 2011, 2 (1): 54-67
(<http://scholarsresearchlibrary.com/archive.html>)



Ti silicide formation by interfacial mixing using swift heavy ion irradiation

Veenu Sisodia, Kailash Baliram Sapnar and Sanjay Dhole

Microtron Accelerator Laboratory, Department of Physics, University of Pune, Pune, India

ABSTRACT

Systematic ion beam irradiation experiments have been performed on titanium- silicon interfaces with 350 MeV energy gold ions at different fluences. Swift heavy ion induced irradiation effects are reported at different fluences from 0.46 to 4.62×10^{14} ions/cm². The samples are characterized before (pristine) and after irradiation using Rutherford Backscattering Spectrometry (RBS) to obtain the depth profiles and the interdiffusion at the interface. X-ray reflectivity measurement was used to study the extent of interfacial mixing. Grazing incidence X-ray diffraction showed the formation of crystalline titanium silicide phase in the mixed zone. The mechanism of SHI beam mixing observed in Ti/Si system is adequately understood by invoking the thermal spike model. Radiation enhanced diffusion was found to be the dominant process in this system. The irradiation effect on the surface roughness of the system is measured using Atomic Force Microscopy (AFM) technique. The current conduction mechanism and schottky barrier height are also calculated by taking I-V curves across the titanium/ Si junction.

INTRODUCTION

Refractory metal silicides such as TiSi, TaSi, MoSi, and WSi, are often considered for application in ultra large- scale integration (ULSI). The materials have been studied extensively due to the combination of the requirements of high-temperature stability, low resistivity and compatibility with current processing steps. Among refractory metal silicides, titanium silicide is considered to be an optimal choice for applications as contacts and interconnects on Si metal-oxide-semiconductor (MOS) devices because the material exhibits the lowest resistivity of the group.

In ULSI technology, silicides are processed in various steps by high temperature thermal treatment (500-1000⁰ C) of thin metal layers deposited on silicon wafers. However, the thermal processing may affect the dopant distribution and device structure [1]. Ion beam technology is able to overcome this limitation as it not only includes silicides at comparatively low

temperature, but also reduces the number of device processing steps. Ion beam mixing has been extensively used in metal-metal [2-6], metal-oxide [7-9] and metal-Si systems [10-14]. Due to their low electrical resistivity and chemical stability, metal silicides are potentially attractive materials in microelectronic devices [15-16] for fabricating contacts, gate electrodes and interconnect. Ion mixing is a well-established technique for the formation of silicide layer. Thus this technique has two advantages: low temperature silicide formation and a reduction of the influence of diffusion barriers. Therefore it was expected in our experiments, that *IBM* process, using swift heavy ions

(*SHI*), having energy >1 MeV, will reduce at such higher energies where the impact of S_n decreases and becomes insignificant while the dominance of S_e increases.

Silicide layers induced by ion mixing have smoother surfaces and better electrical properties compared to those prepared by other techniques [17-18].

IBM is a phenomenon of atomic relocation across an interface under the ion-solid interaction process. The interaction of ions with any material is a decisive factor in ion beam material modification. The ions lose energy during their passage through the material, which is spent in either displacing atoms by elastic collisions (nuclear stopping) or exciting the atoms by inelastic collisions (electronic stopping). The energy loss due to nuclear stopping is called nuclear energy loss S_n , dominant at low energies (keV/amu) and the loss due to electronic stopping is known as electronic energy loss S_e , dominant at high energies (MeV/amu).

Ion beam mixing at the Ni-Si interface was previously investigated [19]. It was observed that over a wide range of irradiation temperatures (10-443K), the thickness of the mixed layer grows in proportion to the squareroot of the dose for 250 keV Ar and 280 KeV Kr irradiations with nearly constant composition. A number of previous studies have been performed on the formation of $TiSi_2$ by thermal annealing route.

In the present study, the formation of $TiSi$ is reported in titanium - silicon (100) system induced by 350 MeV Au ions to a dose of maximum 4.62×10^{14} ions / cm^2 at LN_2 temperature using Rutherford backscattering spectroscopy (RBS), X-ray diffraction (XRD) X-ray reflectivity (XRR), Atomic Force Microscopy (AFM) and electrical measurements.

MATERIALS AND METHODS

2.1 Deposition of films

Silicon wafers were chemically etched by hydrofluoric acid and cleaned before loading in the deposition chamber to remove the native oxide layer from the surface. Titanium layers with a 90 nm thickness were deposited by electron beam evaporation on n-type Si (100) wafers of resistivity 35-72 Ω cm. The top layer was Si (60nm) to avoid oxidation. Titanium of purity 99.98% have been used as a target. The deposition rate was maintained as 0.1 $\text{\AA}/\text{sec}$ at room temperature. The pressure in the chamber during deposition was maintained at $2X 10^{-8}$ m bar.

2.2 Irradiation

The samples were irradiated by 350 MeV Au ions at the LN₂ temperature at three different fluences of $0.46 * 10^{14}$, $1.85 * 10^{14}$ and $4.62 * 10^{14}$ ions/cm² at Helmholtz-Center, Lise Meitner-Campus, Germany. The samples were irradiated uniformly over an area of 1X1 cm². The energy of the ion beam was chosen such that the maximum energy was deposited at the interface of the film and the substrate. The Monte Carlo computer programme TRIM [20] was used to determine the range of ions for the chosen energy.

2.3 RBS technique

Compositional analysis of the sample was done using the Rutherford backscattering technique. These also confirmed the absence of oxygen in the samples. The RBS analysis was performed using 1 MeV He⁺ ions. The spectra were fitted with the help of RUMP computer code [21].

2.4 X-ray technique

X-ray Reflectivity studied structure of the samples.

X-Ray Diffraction in the 2θ scan mode and with the K-α Cu radiation was carried out with a Siemens Diffractometer D5000. As deposited and irradiated samples were studied using XRD to find the presence of any phase or crystal structure at the interface. The difference between X-ray spectra of as deposited and irradiated samples allow separating the irradiation effects created due to heavy ion irradiation.

RESULTS AND DISCUSSION

3.1 RBS studies

The RBS spectra before and after irradiation with 350 MeV Au ions at three different fluences of $0.46 * 10^{14}$, $1.85 * 10^{14}$ and $4.62 * 10^{14}$ ions/cm² at LN₂ temperature, are shown in Fig.1. For clarity we have separated the RBS spectra in to Ti signal (top) and the signals corresponding to the distributions of Si. For increasing ion fluence, it is clearly visible that the Ti yield reduces in height and spreads at the interface. From Fig. 1, we have deduced that Au ion irradiation affect the interface but this can not be seen significantly at lower dose due to the resolution limit of RBS. However for the higher doses, irradiation results in significant mixing as shown in Fig. 1. Indeed, in Fig. 1, for highest dose, a kink detected in the RBS spectrum indicates a phase formation. The simulation of the experimental data using the RUMP programme for the sample irradiated with Au ions revealed the formation of TiSi phase. The RBS simulation shows the mixing of the order of ~ 80 Å. This simulation confirms that the defects are created at high electronic loss, S_e value of Au ions; 31.84 keV/nm in titanium and 19.76 keV/nm in silicon. The fraction of Ti atoms recoiled into Si is higher than that of Si into Ti. Hence we would expect that more Ti atoms move towards the Si, because of this the Ti yield losing at higher fluences. Hence, higher fluences may enable one to observe more transportation of Ti and Si atoms at interface and thus more intermixing. The decrease of Ti backscattered atomic yield in RBS spectra can be explained by taking into account the *IBM* and the compound formation in the form of Ti-silicide, which can explain things accordingly, and it is well documented that when the energy is thermalized between all the local volume atoms, a cascade of high collision density (displacement cascade) zones develops. In this present case both the process ballistic and thermal spike mixing may participate. According to Thermal spike model, the electronic subsystem is excited by the incident ion. It results in high temperature developing transiently

(10^{-5} sec) in the electronic subsystem. The excited electrons rapidly relax by transferring thermal energy to the lattice via electron–phonon interactions.

This generates a thermal spike (≥ 1000 K depending on the ion and solid), in the lattice subsystem for time duration of a fraction of a picosecond to about 100 picosecond. During the transient temperature spike in the lattice, both the layers at the interface reach molten state, go ahead to interdiffusion and hence mixing for both the elements in either side of interface, causing the redistribution of layers in terms of TiSi compound formation.

3.2 X-ray reflectivity studies

In order to examine the surface and interface structure X-ray reflectivity was done. Fig. 2 shows the reflectivity pattern of the samples irradiated at three different fluences. If we compare the reflectivity patterns for the fluences $0.46 * 10^{14}$ and $1.85 * 10^{14}$ ions/cm² there is a shift in the Bragg peaks. Further for the highest fluence, the reflectivity pattern shows a considerable damage at the interface and thus may be attributed to the absence of sharp interfaces between Ti and Si.

3.3 XRD studies

The XRD patterns were carried out using Siemens Diffractometer D 5000 at IUC, Indore, India. Studies were done on the as-deposited and irradiated samples to study the phase formation. The results of the XRD experiments are shown in Fig.3. As deposited sample shows only the metal peaks as Ti [(111), (200)]. For the sample irradiated with lowest fluence i.e. $0.46 * 10^{14}$ ions/cm², shows that the intensity of Ti decreases after irradiation of the sample at this fluence, and this points to a slight diffusion of Ti in Si. Thus there is a change compared to the diffraction pattern of pristine sample as TiSi (210) phase is initiated due to mixing. For the sample irradiated with second highest fluence of $1.85 * 10^{14}$ ions/cm² some additional peaks corresponding to TiSi [(020), (210) and (221)] were observed and $4.62 * 10^{14}$ ions/cm² irradiation shows sharp crystalline peak corresponding to TiSi (210) and other TiSi peaks as TiSi [(020), (030), (221)].

Thus the study revealed that irradiation with Au ions gave rise to the formation of a crystalline silicide phase as revealed by the diffraction peaks located at $2\theta = 35.3529, 35.5608; 54.2843, 54.3309$ and $2\theta = 70.6865, 70.780$ in the diffraction spectra. These peaks were attributed to crystalline TiSi phase.

The bilayer solid phase Ti-Si reaction in the IBM process is as follows: (1) A disorder α -TiSi layer forms at the Ti/Si interface due to interdiffusion of Si and Ti at low fluences. (2) Metastable TiSi phase nucleates at Ti/Si interface and forms an interface layer of TiSi. (3) The TiSi layer grows vertically to the surface of the sample as silicon diffuse through the TiSi layer to react with the overlying Ti layer and TiSi phase nucleated along the layer and grows rapidly. Thus the mixing has been assumed to have taken place due to interdiffusion in transient melt phase of the latent tracks. The result shows that extensive Si interdiffusion into Ti occurs at highest fluences. The interdiffusion precedes silicide compound formation.

This work is focused on the titanium silicide formation. The process is typical of the requirement of forming contacts on source and drain regions which would result in intermixing of Ti with Si. Therefore one expects the TiSi₂ phase with C49 structure and low resistivity C54 structure. In

this study, a film thickness of 90 nm of Ti, after irradiation, leads to the formation of TiSi phase. Thus we suggest that, even at high ion energies, intermixing depends on the phase that first nucleates in to the system as a result of ion irradiation. With such a strong e-p coupling, the huge amount of electronic energy deposited by incident Au ions is efficiently transferred to the lattice, causing radiation damage, atomic displacement and consequent mixing of Ti and Si. Interdiffusion occurs at the metal-Si interface during

There will be reaction driven diffusion across the interface, once reaction is initiated. The source of semiconductor atoms is sufficient to satisfy mass balance, a single phase described by the equation $xM + yS = M_xY_s$ will form. Where x and y denotes the number of metal and semiconductor atoms M and S, respectively. On the other hand, a second reaction product will form when semiconductor atom diffusion through the reacted overlayer is unable to balance the number of metal atoms arriving at the surface. Two reacted species can form simultaneously because the interface is morphologically heterogeneous. In modeling this reaction, it is necessary to partition the arriving metal atoms between the two phases. This has been approximated by a linear lever rule [22],

$$X = (\theta - \theta_2) / (\theta_1^* - \theta_2),$$

Where θ is the metal coverage, θ_2 is the coverage at which the second phase starts to form and θ_1^* is the coverage at which the first phase stops. This process assumes that each reaction product has a distinct stoichiometry. As in the present study TiSi phase is nucleated in the interdiffusion region. These results add further to those previously published [23-25].

3.4 AFM studies

High energy Au ion induced irradiation effects at the surface of the Ti/Si system were observed by using Atomic Force Microscope in our institute. AFM measurements provide a closer look to the features and roughness that emerged on the top surfaces after *SHI* irradiation. For the surface morphology of all samples the scanning area was kept as $2 \mu\text{m} \times 2 \mu\text{m}$. The AFM micrographs are shown in Fig.4, for both for the unirradiated and irradiated ones. The observed features are very interesting which show a clear granular feature on the top face of silicon on which the metal film was deposited and irradiation was also done on it. The grains seem to be embedded in the layer below the surface. The features show oriented granular structure which looks like an open face spherical ball. With the increasing ion dose roughness at the surface increases as the granular structures agglomerate and the grain size also increases. The observed structure clearly shows that there is a strong irradiation induced intermixing.

3.5 I-V studies

The electronic transport across such Schottky contacts is characterized by their barrier height, which is equal to the difference between electron affinity of semiconductor and the work function of metal. For electrical characterization, I V measurements were taken using four probe techniques in our laboratory by applying silver paste on top and bottom to make contact on the sample. DC characterization of the device for the purposes of performance analysis and parameter extraction is shown in Fig. 5.

As deposited Metal/Semiconductor contacts usually exhibit non-ideal (rectifying) current-voltage characteristics. The current transport through the device by emission over the barrier is essentially a two step process. 1.) The electrons have to be transported through the depletion region and this is determined by the usual mechanisms of diffusion and drift and 2.) An electron must undergo emission over the barrier into the metal and this is controlled by the number of electrons that impinge on unit area of the metal per second, which gives:

$$I = AA^*T^2 \exp\left(\frac{-q\phi_b}{kT}\right) \left(\exp\left\{\frac{-qV_{\text{eff}}}{nkT}\right\} - 1\right) \quad (1)$$

where A is the cross-sectional area of the Metal/Semiconductor interface, A^* the effective Richardson constant for the Metal/Semiconductor interface, given as $A^* = [(4\pi m^* k^2 e) / h^3] = 31.2 \text{ A/cm}^2 \text{K}^2$, T the temperature in Kelvins, k the Boltzmann constant, q electronic charge, V_{eff} the effective bias across the interface, n the ideality factor, m^* effective mass of the conduction electrons in Si ($= 0.26m_0$), h Planck's constant and m_0 the rest mass of electron.

In the present case current transport dominated by thermionic emission is assumed. We resolved (1) for a straight line equation, in a way to plot $\log I$ on the y-axis and V_{eff} or applied bias on the x-axis to obtain the intercept at y-axis in terms of saturation current, from the semilogarithmic I-V curve shown in Fig. 5 (b). From equation (1) the calculated saturation current I_s is:

$$I_s = AA^*T^2 \exp\left(\frac{-q\phi_b}{kT}\right) \quad (2)$$

Thus the barrier height is

$$\phi_b = \frac{kT}{q} \ln\left(\frac{AA^*T^2}{I_s}\right) \quad (3)$$

Table I Table of calculated Schottky barrier height at different irradiation fluences

Irradiation fluence	Interface reacted silicide	SBH (eV)
Unirradiated	—	0.612
0.46×10^{14} ions/cm ²	TiSi	0.601
1.85×10^{14} ions/cm ²	TiSi	0.600
4.62×10^{14} ions/cm ²	TiSi	0.515

To calculate the value of I_s , we extract the y-axis intercepts for each curve. Taking the value of I_s from I-V curve and calculating the value of effective Richardson constant as $31.2 \times 10^4 \text{ Amp/m}^2 \text{K}^2$ (by taking the effective mass of the conduction electrons in Si, $m^* = 0.26m_0$) the calculated values of the Schottky Barrier Height (SBH) for different samples are summarized in Table I. It can be seen from the table that at lower fluence irradiation the barrier height is about unchanged in reference of unirradiated sample but at the highest fluence, 4.62×10^{14} , the barrier height decreases sharply, which indicates the formation of some new phase (TiSi) at the interface.

Since metal-disilicides are stable phases in the Periodic table, TiSi is not the stable phase but its disilicide TiSi_2 is stable. It is well established that S_n causes creation of defects like vacancies, interstitials, etc. at the interface and this will lead to an increase in the interface state density DS. *SHI* irradiation results in the introduction of interface states at MS (Metal/Si) interface which influence the SBH.

From I–V characteristics for an unirradiated sample we have calculated the SBH as 0.612 eV. When irradiated at a fluence of 0.46×10^{14} ions/cm² and 1.85×10^{14} ions/cm², SBH is almost same as the unirradiated one, and shows no more change in the interface state density. While for the fluence 4.62×10^{14} ions/cm², the SBH is found to be decreased. According to the Fermi level pinning model of Bardeen [26], when the interface state density increases schottky limit to Bardeen limit, the SBH decreases. One thereby concludes that SHI irradiation at high fluence causes an increase in interface state density at the MS interface leading to decrease in SBH with the formation of TiSi.

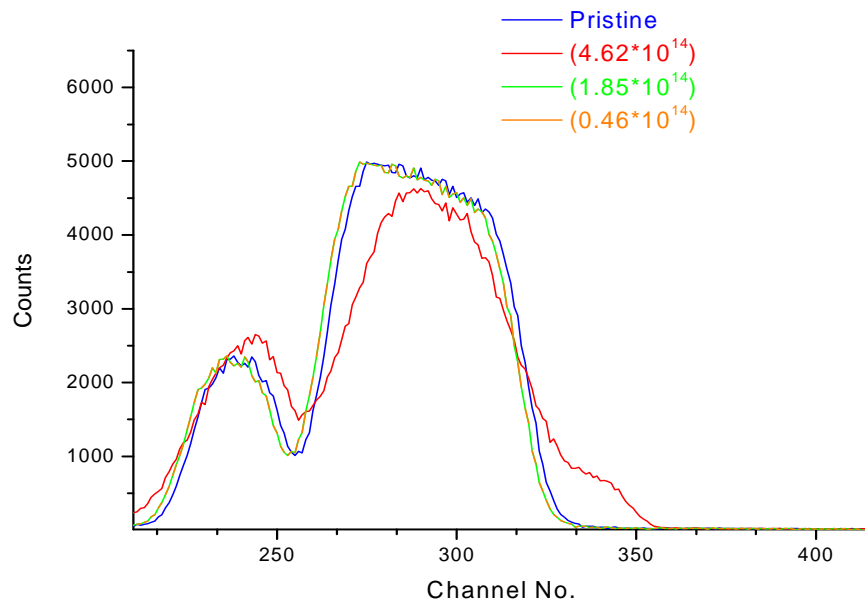


Fig.1 (a) RBS spectra of titanium, taken before and after ion irradiation with 350 MeV Au ions at fluence of $(0.46-4.62) \times 10^{14}$ ions/ cm²

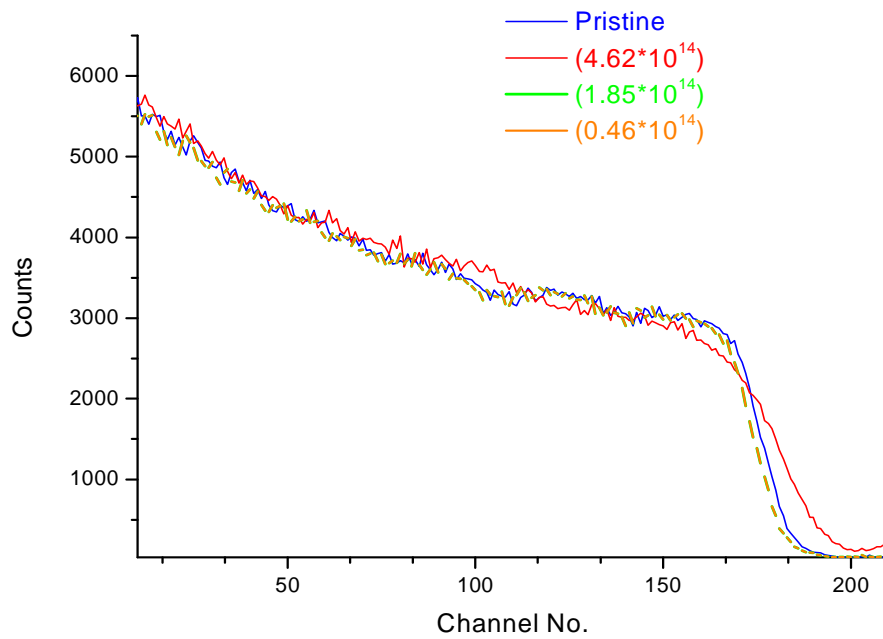


Fig.1 (b) RBS spectra of silicon, taken before and after ion irradiation with 350 MeV Au ions at fluence of $(0.46-4.62) \cdot 10^{14}$ ions/cm²

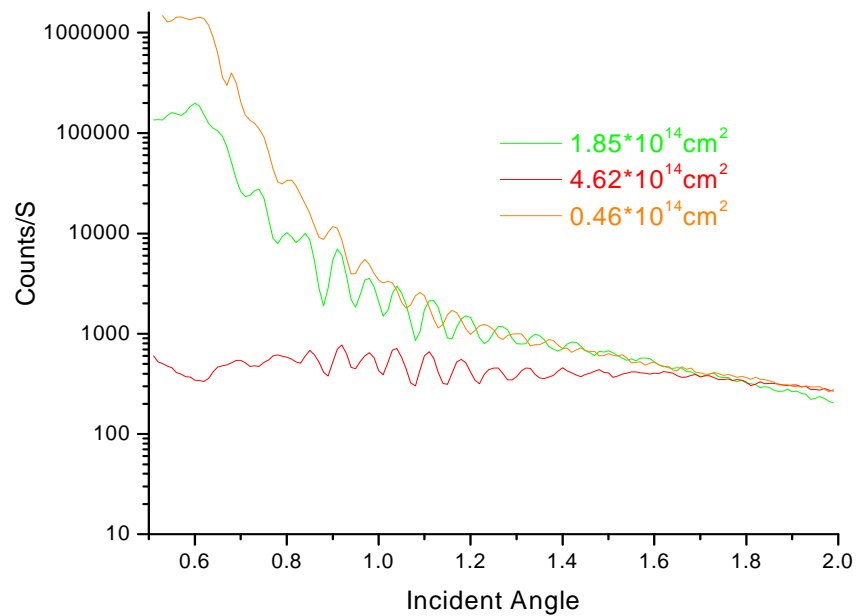


Fig. 2 XRR spectra of pristine and Au (350 MeV, $0.46 \cdot 10^{14}$, $1.85 \cdot 10^{14}$ and $4.62 \cdot 10^{14}$ ions/cm²) irradiated specimen

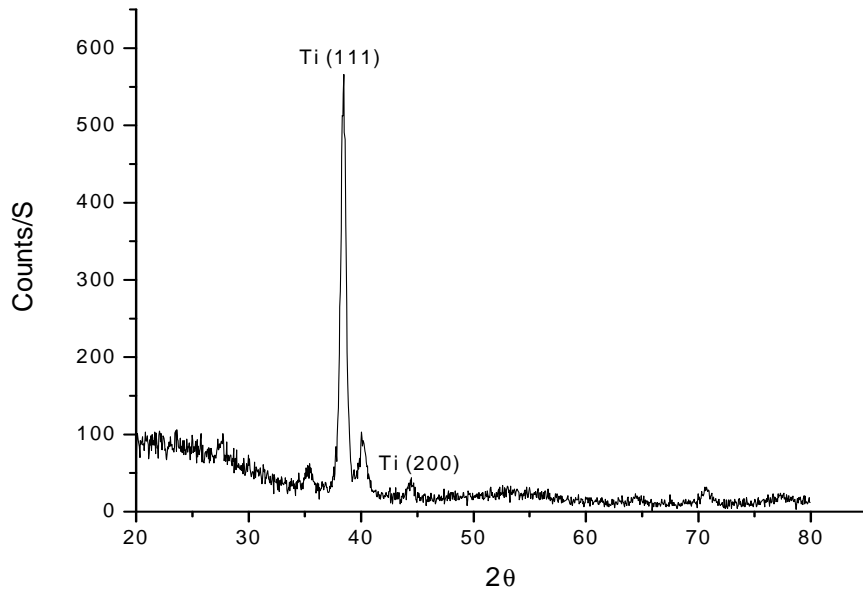


Fig.3 (a)

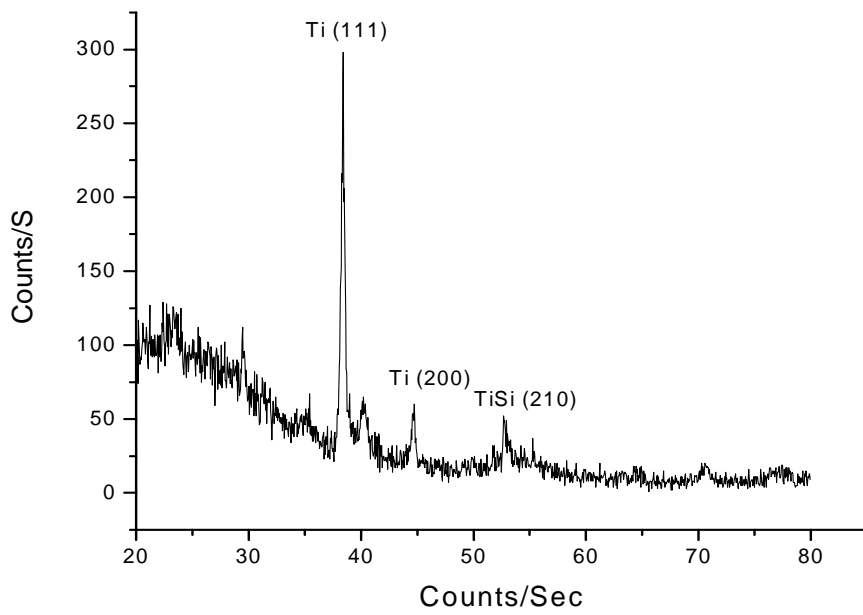


Fig.3 (b)

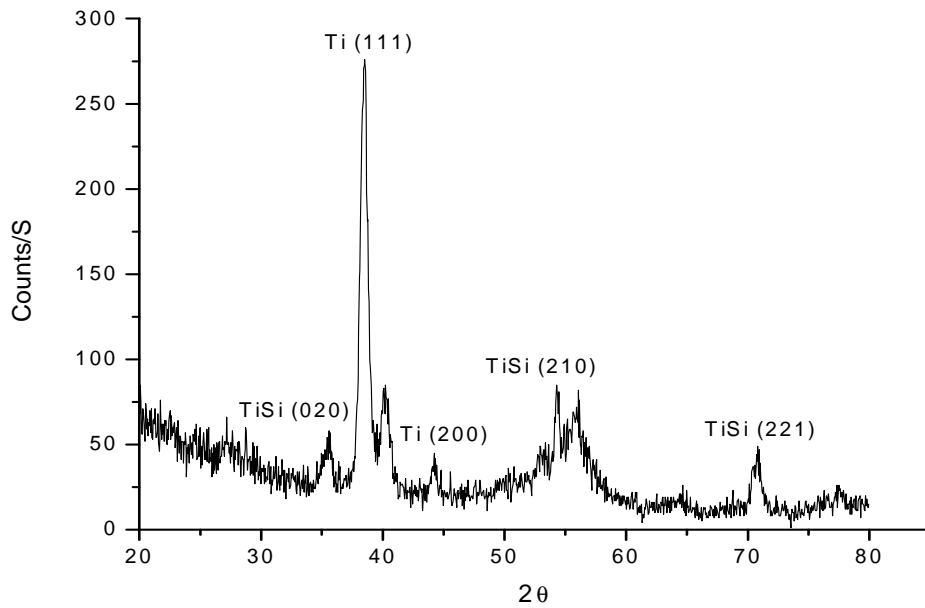


Fig.3 (c)

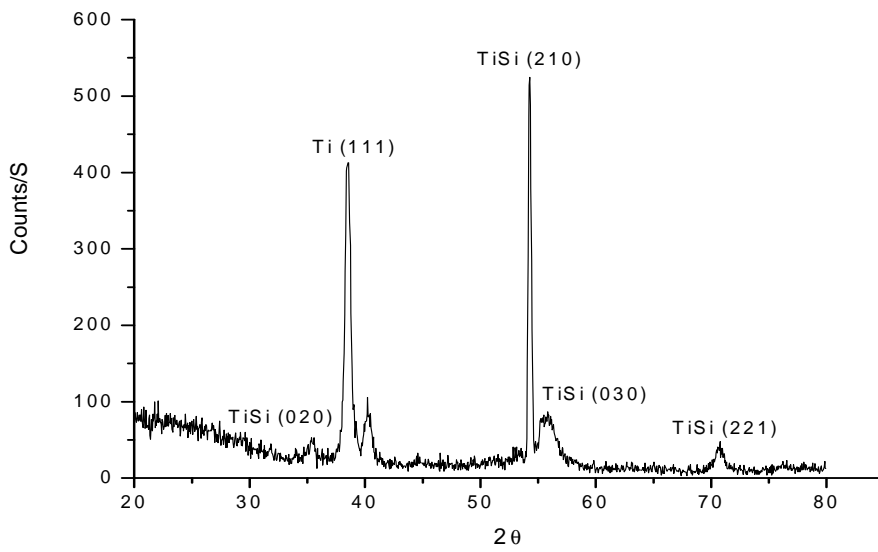


Fig.3 (d)

Fig. 3 GIXRD spectra of Ti/Si specimen
 (a) pristine
 (b) Au (350 MeV, $0.46 \cdot 10^{14}$ ions/ cm^2) irradiated
 (c) Au (350 MeV, $1.85 \cdot 10^{14}$ ions/ cm^2) irradiated
 (d) Au (350 MeV, $4.62 \cdot 10^{14}$ ions/ cm^2) irradiated

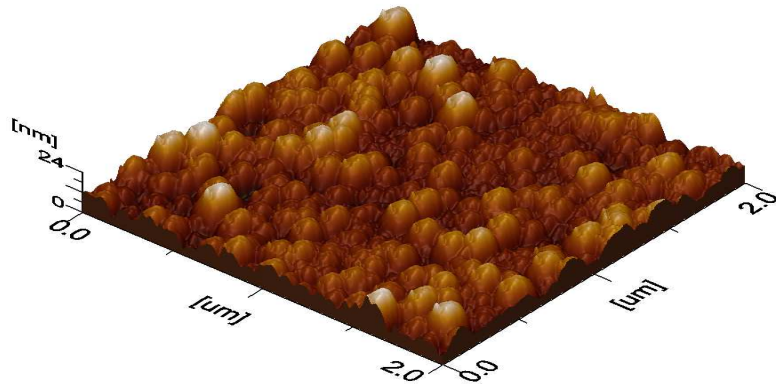


Fig.4 (a)

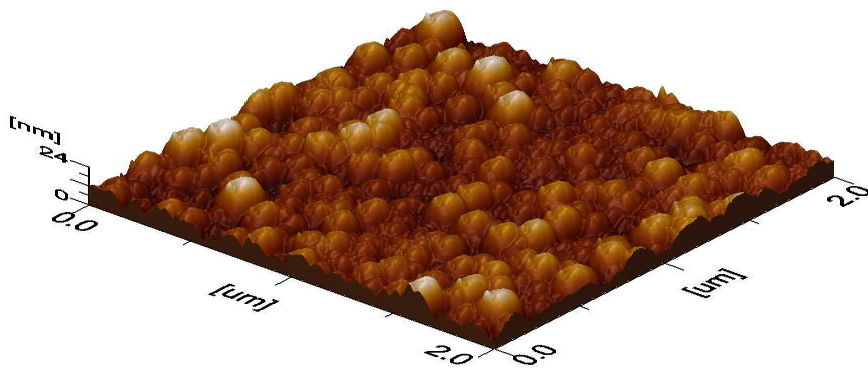


Fig.4 (b)

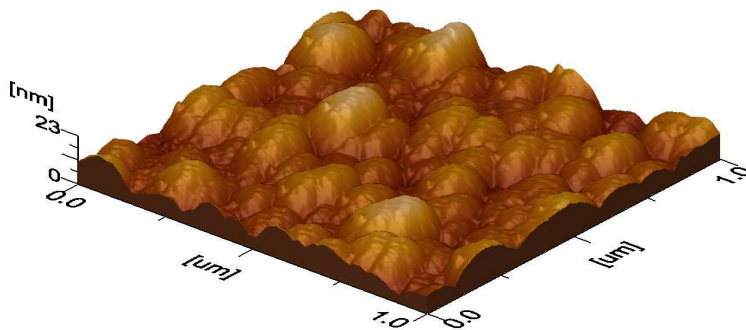


Fig.4 (c)

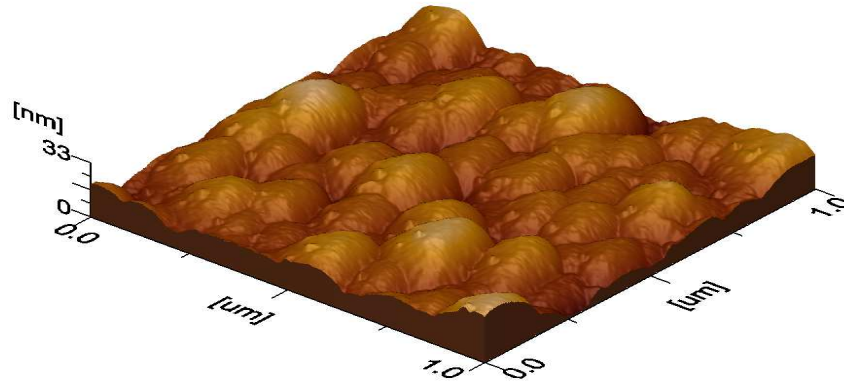


Fig.4 (d)

Fig. 4 AFM images in 3D view of Zr/Si thin films

- (a) pristine
- (b) irradiated at fluence 0.46×10^{14} ions/cm²
- (c) irradiated at fluence 1.85×10^{14} ions/cm²
- (d) irradiated at fluence 4.62×10^{14} ions/cm²

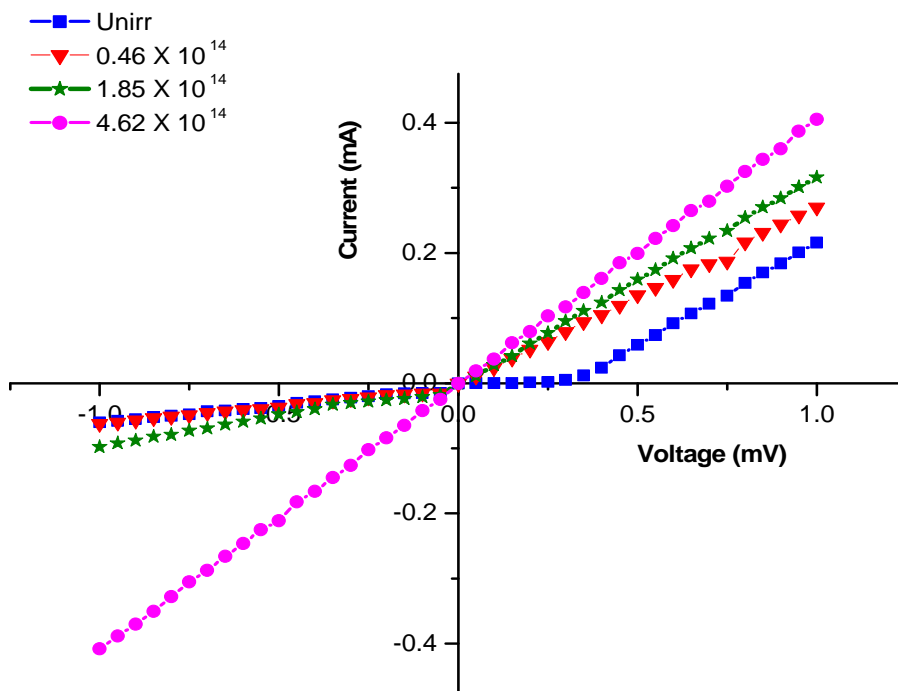


Fig.5 (a) I-V curve of unirradiated and irradiated Zr/Si thin films at fluences 0.46×10^{14} , 1.85×10^{14} and 4.62×10^{14} ions/cm²

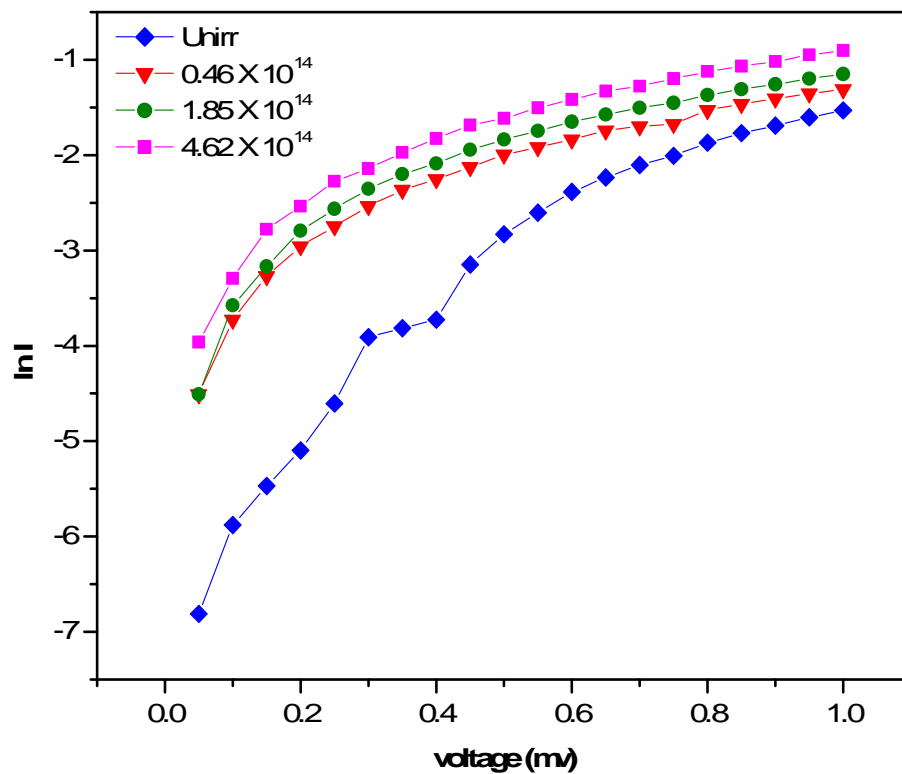


Fig.5 (b): Semi-logarithmic I-V curve of unirradiated and irradiated Zr/Si thin films at fluences 0.46×10^{14} , 1.85×10^{14} and 4.62×10^{14} ions/cm²

CONCLUSION

We have measured the schottky barrier height of the silicide of refractory metal Ti and studied the ion beam mixing of Ti-Si bilayers using a high-energy heavy ion irradiation. The result shows that the type of silicide forms has only a small effect on the barrier height. We have noted the formation of TiSi phase exhibits almost similar SBH as for the stable TiSi₂ phase, studied widely. The barrier height of the silicide decreases with the increasing ion dose and the results are consistent with the predictions of recent models of barrier formation based on Fermi-level pinning in the centre of the indirect band gap.

Acknowledgement

It is our pleasure to acknowledge the technical group in making irradiation and RBS done in Berlin, Germany. Thanks to the University Grants Commission, New Delhi, India for releasing funds for the present research work.

REFERENCES

- [1] N.Boussa: *Vacuum* 77 (2005) 125.
- [2] M.Natasi and J.W.Mayer: *Mat Sc Eng R12* (1994) 1.
- [3] W.Bolse: *Mat Sc Eng A* 253 (1998) 194.

-
- [4] B.X.Lau: *Phys Stat Sol (a)* 94 (1996) 11.
- [5] Y.T.Chang: *Mat Sc Rep* 5 (1990) 45.
- [6] F.Shi, W.Bolse and K.P.Lieb: *J Appl Phys* 78 (1995) 2303.
- [7] C.J.McHargue, D.L.Joslin and C.W.White : *Nucl Instr Meth B* 91 (1994) 549.
- [8] S.K.Sinha, D.C.Kothari, T.Som, V.N.Kulkarni, K.G.M.Nair and M.Natali: *Nucl Instr Meth B* 170 (2000) 120.
- [9] S.Kraft, B.Schattat, W.Bolse, S.Klaumunzer, F.Harbsmeier, A.Kulinska and A.Loffi: *J Appl Phys* 91 (2002) 1129.
- [10] W. Bolse: *Mat Sc Eng R* 12 (1994) 53.
- [11] P.I.Gadiuk, F.F.Komarov, A.Witzmen, A.Zentdruf and S. Shipel :*Nucl Instr Meth B* 94 (1994) 231.
- [12] N.Bibic, S.Dhar, M.Milosavljevic, K.Removic, L.Rissanen and K.P.Lieb: *Nucl Instr Meth B* 161/163 (2000) 1011.
- [13] D.K.Sarkar, S.Dhara, M.Milosavljevic, K.Removic, L.Rissanen and K.P.Lieb: *Nucl Instr Meth B* 168 (2000) 21.
- [14] M.Milosavljevic, S.Dhar, P.Schaff, N.Bibic, Y.L.Huang, M.Seibt and K.P.Lieb: *J Appl Phys* 90 (2001) 4474.
- [15] F.M.d'Heurle: P.J.Was, *Matter Res* 1 (1986) 205.
- [16] A. Baba, H.Aramaki, T.Sadoh and T.Tsurushima: *J Appl Phys* 82 (1997) 5480.
- [17] C.J.Mchargue, G.C.Parlow, C.W.White, J.M.Williams, B.R.Appleton and H.Naramato: *Mat Sci Eng* 69 (1985) 123.
- [18] W.L.Johnson, Y.T.Cheng, M.Van Rossum and M.A. Nicolet: *Nucl Instr Meth B* 53 (1985) 1342.
- [19] R.S.Averback, L.J.Thompson, Jr. J.Moyle and M.Schalit: *J Appl Phys* 53 (1982) 1342.
- [20] J.F.Zeigler, J.P.Biersack and U.Littmark: *The stopping range of ions in solids*, Pergamon, New York (1985).
- [21] L.R.Doolittle: *Nucl Instr Meth B* 9 (1985) 344.
- [22] R.A. Butera, M.D. Guidice and J.H.Weaver: *Phys. Rev.B* 33 (1986) 5435.
- [23] V.Sisodia: *Rad. Meas* 36 (2003) 657.
- [24] M.Bhaskaran, S.Sriram, K.T. Short, D.R.G. Mitchell, A.S. Holland and G.K. Reeves: *J Phys D* 40 (2007) 5213.
- [25] V.Sisodia, *Appl Sur Sc* 252 (2006) 4016.
- [26] J.Bardeen, *Phys Rev* 71 (1947) 717.